THE JOURNAL OF BIOLOGICAL CHEMISTRY VOL. 283, NO. 34, pp. 23315–23325, August 22, 2008

Crystal Structure of the Cold-active Aminopeptidase from *Colwellia psychrerythraea*, a Close Structural Homologue of the Human Bifunctional Leukotriene A_4 Hydrolase*[S]

Received for publication, March 18, 2008, and in revised form, May 28, 2008 Published, JBC Papers in Press, June 6, 2008, DOI 10.1074/jbc.M802158200

Cédric Bauvois[‡], Lilian Jacquamet[§], Adrienne L. Huston[¶], Franck Borel[§], Georges Feller[¶], and Jean-Luc Ferrer[§1]

From the [‡]Institut de Recherche Microbiologique J.-M. Wiame, Laboratoire de Microbiologie, Université Libre de Bruxelles, 1 rue E. Gryson, B-1070 Bruxelles, Belgium, [§]Laboratoire de Cristallographie et Cristallogenèse des Protéines, Institut de Biologie Structurale J.-P. Ebel, CEA-CNRS-Université Joseph Fourier, 41 rue Jules Horowitz, F-38027 Grenoble cedex 1, France, and [¶]Laboratoire de Biochimie, Institut de Chimie B6a, Université de Liège, Sart-Tilman Campus, B-4000 Liège, Belgium

The crystal structure of a cold-active aminopeptidase (ColAP) from *Colwellia psychrerythraea* strain 34H has been determined, extending the number of crystal structures of the M1 metallopeptidase family to four among the 436 members currently identified. In agreement with their sequence similarity, the overall structure of ColAP displayed a high correspondence with leukotriene A4 hydrolase (LTA4H), a human bifunctional enzyme that converts leukotriene A4 (LTA4) in the potent chemoattractant leukotriene B4. Indeed, both enzymes are composed of three domains, an N-terminal saddle-like domain, a catalytic thermolysin-like domain, and a less conserved C-terminal α-helical flat spiral domain. Together, these domains form a deep cavity harboring the zinc binding site formed by residues included in the conserved HE*XX*HX_{18}H motif. A detailed structural comparison of these enzymes revealed several plausible determinants of ColAP cold adaptation. The main differences involve specific amino acid substitutions, loop content and solvent exposure, complexity and distribution of ion pairs, and differential domain flexibilities. Such elements may act synergistically to allow conformational flexibility needed for an efficient catalysis in cold environments. Furthermore, the region of ColAP corresponding to the aminopeptidase active site of LTA4H is much more conserved than the suggested LTA4 substrate binding region. This observation supports the hypothesis that this region of the LTA4H active site has evolved in order to fit the lipidic substrate.

It is generally accepted that thermal adaptation of proteins is correlated with changes in their overall or local structure flexibility. Indeed, although thermophilic enzymes are characterized by a relatively high rigidity, their psychrophilic homologues display molecular characteristics enhancing their plasticity. The current understanding is that this increased flexibility, by enhancing accommodation and transformation of their substrates, allows psychrophilic enzymes to be active at low temperature. To identify features that may be important for cold adaptation, the ColAP[2] structure was analyzed and compared in detail with one of its closest structural homologues, the human mesophilic leukotriene A4 hydrolase (LTA4H).

A recent study (1) revealed a high sequence similarity (34% identity and 56% similarity) between cold-active aminopeptidase ColAP and LTA4H. Both enzymes belong to the M1 metallopeptidase family that includes enzymes such as aminopeptidase N (APN), pyroglutamyl-peptidase II, and aminopeptidase A. Interestingly, human LTA4H has the particularity of being bifunctional. Indeed, this enzyme is also an epoxide hydrolase and catalyzes the conversion of leukotriene A4 (LTA4) in LTB4, a chemoattractant implicated in inflammatory mechanisms. Although it is well known that both reactions occur in the same unique active site (2), the molecular features that make LTA4H bifunctional, even though their homologues are not, are still unknown. In this article, we report the crystal structure of cold-adapted ColAP. This structure has been compared with the three-dimensional structure of its close mesophilic homologue LTA4H, solved at 1.95 Å (3). Such a study may help not only to improve our understanding of molecular properties leading to cold-adaptation of this enzyme but also to indicate the structural differences that allow the human enzyme to have a second catalytic function.

EXPERIMENTAL PROCEDURES

Protein Purification—Recombinant ColAP was overproduced in *Escherichia coli* and purified as described previously (4).

Crystallization—Crystals of ColAP were obtained after a 1-week incubation at 18 °C by using the hanging drop method.

* This work was supported by the Commissariat à l'Energie Atomique (France), the Centre National pour la Recherche Scientifique (France), and grants from the Fonds National de la Recherche Scientifique, Belgium (to G. F.) and the National Science Foundation (to A. L. H.). The costs of publication of this article were defrayed in part by the payment of page charges. This article must therefore be hereby marked "*advertisement*" in accordance with 18 U.S.C. Section 1734 solely to indicate this fact.

[S] The on-line version of this article (available at http://www.jbc.org) contains supplemental Table 1.

The atomic coordinates and structure factors (code 3CIA) have been deposited in the Protein Data Bank, Research Collaboratory for Structural Bioinformatics, Rutgers University, New Brunswick, NJ (http://www.rcsb.org/).

[1] To whom correspondence should be addressed: Laboratoire de Cristallographie et Cristallogenèse des Protéines, Institut de Biologie Structurale J.-P. Ebel, CEA-CNRS-UJF, 41 rue Jules Horowitz, F-38027 Grenoble cedex 1, France. Tel.: 33-4-38-78-59-10; Fax: 33-4-38-78-51-22; E-mail: jean-luc.ferrer@ibs.fr.

[2] The abbreviations used are: ColAP, *Colwellia psychrerythraea* aminopeptidase; LT, leukotriene; LTA4H, human leukotriene A_4 hydrolase; APN, aminopeptidase N; bis-Tris, 2-[bis(2-hydroxyethyl)amino]-2-(hydroxymethyl)-propane-1,3-diol; r.m.s.d., root mean square deviation; GRAVY, grand average of hydropathy.

TABLE 1

Crystallographic data and refinement statistics

Values in parentheses are for the outer resolution shell.

X-ray diffraction data	
Space group	P1
Resolution range (Å)	46.7–2.7 (2.87–2.7)
Cell parameters	a = 81.37 Å, b = 87.1 Å, c = 116.4 Å, α = 88.8°, β = 70.7°, γ = 88.4°
Unique reflections	82,772
Completeness (%)	97.28 (96.7)
I/σ	7.27 (2.61)
R_{pim} (%)[a]	9.3 (38.1)
R_{rim} (%)[b]	14.2 (57.1)
Refinement	
Protein atoms	18,697
Solvent molecules	919
R_{cryst} (%)[c]/R_{free} (%)[d]	24.8/26.7
Average B-values for protein (Å^2)	32.2
r.m.s.d. of bonds (Å)/angles (degrees)	0.026/2.28
Ramachandran plot[e]	86.4/98.8/1.2

[a] $R_{pim} = \Sigma_{hkl}[1/(n-1)]^{1/2} \Sigma_i|I_i(hkl) - \langle I(hkl)\rangle|/\Sigma_{hkl}\Sigma_i I_i(hkl)$ (7, 8).
[b] $R_{rim} = \Sigma_{hkl}[n/(n-1)]^{1/2} \Sigma_i|I_i(hkl) - \langle I(hkl)\rangle|/\Sigma_{hkl}\Sigma_i I_i(hkl)$ (7, 8).
[c] $R_{cryst} = \Sigma||F_{obs}| - |F_{calc}||/\Sigma|F_{obs}|$.
[d] 5% of the data were set aside for the R_{free} calculation.
[e] Percentage of residues in favored/allowed/disallowed regions of the Ramachandran plot. Ramachandran results were determined by using MOLPROBITY (14).

Optimal crystallization conditions were obtained by mixing the protein with an equal volume of reservoir solution composed of polyethylene glycol 3350 (23% w/v), NaCl 0.5 M, and bis-Tris 0.1 M, pH 6.5.

Structure Determination and Refinement—Diffraction data were collected at the FIP beamline (French beamline for Investigation of Proteins; BM30A) (5) of the European Synchrotron Radiation Facility (ESRF, Grenoble, France) at 100 K. The data set was processed using the XDS program (6). The precision-indicating merging *R*-factor (R_{pim}) and the redundancy-independent merging *R*-factor (R_{rim}) were calculated using RMERGE (7, 8) (Table 1).

The native data set was used for molecular replacement, with the structure of LTA4H as a starting model (Protein Data Bank code 1HS6). Four molecules were found in the asymmetric unit. The electronic density was good enough to build a first model manually using the programs O and COOT (9, 10). Then, this first model was subjected to standard simulated annealing using a protocol of torsional dynamics refinement, as implemented in the CNS suite (11), followed by energy minimization using the REFMAC5 program (12).

Structure and Sequence Analysis—Sequence analysis and GRAVY and aliphatic indexes were computed with ProtParam (13) tools from the ExPASy proteomics server. Structure quality was evaluated with MOLPROBITY (14) and WHAT CHECK (15). Polar and apolar exposed surfaces were calculated with the DSSP program (16), and hydrogen bonds were defined using HBPLUS software (17). Ion pairs were identified as two oppositely charged residues (considering Asp, Glu, Lys, and Arg) having their charges located within 4 Å. Structure superimpositions were performed using DEEPVIEW (18). All figures have been generated using PyMOL.

RESULTS AND DISCUSSION

Overall Structural Comparisons—As expected from the high sequence similarity, the overall fold and the main secondary structures of ColAP are very similar to those of LTA4H (Fig. 1, *b* and *c*). The backbone structures of both enzymes can be superimposed with a root mean square deviation (r.m.s.d.) of 1.21 Å for 509 Cα. These monomeric enzymes are folded into three distinct domains (N-terminal, catalytic, and C-terminal domains) in which the topologies are largely conserved. The N-terminal domain comprises three β-sheets, the major one consisting of seven mixed β-strands and two minor ones consisting of three and four antiparallel β-strands, respectively. Small β-sheets are located under the large sheet at opposite extremities. On the whole, N-terminal domain β-sheets resemble a kind of saddle, presenting its large concave surface to the solvent. As already observed for LTA4H, the architecture of the ColAP catalytic domain is similar to that of thermolysin. It comprises two lobes: one is composed of α-helices only, whereas the other is a mix of α-helices and β-strands. Between the lobes, a depression contains the zinc binding site. The C-terminal domain of ColAP is α-helical. In this domain, eight successive helices are arranged in a right-handed flat spiral. Helices are situated in two layers, five in the inner layer and three in the outer layer, respectively. In the LTA4H enzyme, there is a Pro-rich loop located between the catalytic and C-terminal domains. The sequence of this loop (^{453}LPPIKP^{458}) resembles the Src homology 3-binding domains (*X*Pp*X*P, where *X* is an aliphatic residue, P is a conserved proline, and p is sometimes a proline) (19). In ColAP, the corresponding sequence is ^{480}LPSYAP^{485} and thus is moderately conserved. Of the three domains of ColAP and LTA4H, the least conserved is the C-terminal domain. The greatest sequence variations are indeed found in this domain (18% identity for the C-terminal domain *versus* 38 and 41% for the N-terminal and catalytic domains, respectively) (supplemental Table 1). These differences are reflected in the r.m.s.d. between Cα atoms of the domain structures. Superimposition of the different domains of ColAP and LTA4H gives r.m.s.d. values of 0.83, 1.15, and 1.63 Å based on 716, 920, and 440 involved atoms for the N-terminal, catalytic, and C-terminal domains (supplemental Table 1).

Other enzymes share a similar overall fold, such as the Tricorn protease-interacting factor 3 from *Thermoplasma acidophilum* (20) and the APN from *E. coli* (21). Although APN shares the three equivalent domains described for ColAP and LTA4H, Tricorn protease contains an additional small barrel-like β-structure domain located between the catalytic and C-terminal domains. Interestingly, in these two enzymes the major differences are also found in the C-terminal domains. The discrepancies are so significant that backbone superimposition could not be performed with ColAP.

Amino Acid Distribution and Cold Adaptation—A comparison of the amino acid composition of the psychrophilic ColAP with its mesophilic human homologue is shown in Table 2. Although the hydrophobic amino acid content is similar for both enzymes, the number of Ala residues is much higher in ColAP. Interestingly, this increase (~3.2%) seems to compensate for the decrease observed for Ile, Leu, and Pro residues (~3.1%). Ala is less hydrophobic than Ile and Leu and less constraining for the backbone than Pro, which suggests a global gain in structure flexibility. The high Ala content and the small side chain of this residue may also contribute to the reduction of the global volume of the psychrophilic ColAP.

Table 2 also reveals the substitution of glutamic acid by aspartic acid in ColAP. This is in agreement with the trend observed in the whole genome of *Colwellia psychrerythraea* (22). By contrast, the Asp content in thermophilic proteins is low, and it has been shown that Asp has less favorable conformational entropy in stability than Glu (23). Accordingly, the high Asp content in ColAP may contribute to its lower stability and higher flexibility. The Pro content is also significantly lower in ColAP. Five of these substituted Pro residues are located in loops, three in α-helices and two in β-strands in the mesophilic homologue LTH4A. In the latter structure, Pro-511 adopts the *cis*-conformation whereas in ColAP all Pro are in *trans*-conformation. The replacement of these Pro by residues possessing a larger dihedral angle probably contributes to the increase in backbone flexibility in ColAP.

Other variations in the amino acid content can be also influenced by the cold environment. Indeed, ColAP is characterized by a higher Asn content. A similar trend has been observed in the whole genome of another psychrophilic bacterium, *Pseudoalteromonas haloplanktis* TAC125 (24). This residue is involved in protein aging, as the Asn side chain is heat-labile and prone to deamination at high temperatures (23). In a cold environment, this feature is not under strong selective pressure, which may explain the increased Asn content in the cold-adapted enzyme. The absence of Cys in ColAP may also be related to the environment of *C. psychrerythraea.* Indeed, cold aerobic environments are more oxidative, as oxygen solubility increases at low temperatures. As ColAP enzyme is secreted in the external medium in a temperature range of −1 to 10 °C, natural selection may have led to the lack of Cys.

The GRAVY and aliphatic indexes are computed parameters related to global hydrophilicity and hydrophobicity of proteins. These indexes are often lower for cold-adapted enzymes as compared with their mesophilic or thermophilic homologues. Actually, the values obtained from the GRAVY index, isoelectric point, and aliphatic index of ColAP are lower than those for LTA4H. Both of the former parameters can be tentatively related to better interactions with the solvent (25), whereas the latter (the aliphatic index) suggests a lower hydrophobic effect stabilizing the core of ColAP.

Loop and Secondary Structure Variations—An extension of the enzyme loop regions has been suggested as a possible determinant in cold-adaptation, as their increased lengths and less constrained conformations should lead to an increase in the conformational entropy of psychrophilic proteins (26). However, one should keep in mind that the delimitation of secondary structures is also related to the preciseness of the atomic position and, as a consequence, is linked to the resolution of the crystallographic data. From our point of view, such an analysis needs to be considered carefully when comparing two different structures, and only general trends should be interpreted as thermally related parameters. An analysis of ColAP secondary structures revealed a striking increase in the loop content as compared with LTA4H. Indeed, the relative residue content in the loop, helices, and strand was found to be 47 *versus* 38%, 31 *versus* 38%, and 22 *versus* 24% in ColAP *versus* LTA4H. The additional 9% in loop content, 2, 3, and 4% was found in the N-terminal, catalytic, and C-terminal domains, respectively. Interestingly, although globally the regular secondary structures are shorter in ColAP (with 68 additional residues adopting a loop conformation), the loops conserved in both enzymes are shorter in the human enzyme. This clearly indicates that the increased loop content observed in ColAP corresponds mainly to a shortening of the regular secondary structures and not to insertions in exposed loops. The α-helix content is more affected than the β-strand content; about two-thirds of the residues concerned are situated in α-helices, whereas only one-third are located in β-strands in LTA4H. Interestingly, based on structural genomics studies, the inverse effect has been observed in thermophilic proteins, as a decrease in the overall loop content was found to be correlated to an increase in helical content (27). As seen from Table 3, the global higher loop content of ColAP is correlated with a larger proportion of loops exposed to the solvent. In ColAP, the total accessible surface of the loops is 9% higher as compared with LTA4H. The GRAVY index of secondary structures (Table 2) indicates that loops tend to be more hydrophilic in ColAP. In addition, the backbones of the exposed loops in ColAP are generally less implicated in hydrogen bonding to each other and therefore favor interactions with water molecules. Altogether, these observations suggest that ColAP, by having a higher loop content exposed to the solvent, has improved the breathing (or micro-unfolding) of its external shell in comparison with its mesophilic counterpart.

In addition to the above mentioned size reduction of α-helices in ColAP, charge stabilization of the helix macrodipole, generated by the helical alignment of polarized peptide bonds, is weakened in the psychrophilic enzyme. Considering for instance the charges present in the first turn and on the N-cap of all helices, ColAP displays nine favorable (negative) and four unfavorable (positive) charges, whereas the human enzyme possesses 11 favorable and only two unfavorable charges at the helix N termini. Such weakening of the macrodipole in ColAP is thought to reduce the compactness of helices, originating from local microdipole alignment.

Finally, it should be noted that no electron density was found for the first 13 amino acid residues of ColAP. This suggests that the N terminus of the psychrophilic enzyme has a weakly defined structure in the solvent. As a matter of fact, the N- and C-terminal extremities of cold-adapted proteins are frequently less constrained when compared with their mesophilic or thermophilic homologues (28). As these relaxed extremities are preferential sites for unfolding, they may contribute to the global destabilization strategy in psychrophilic enzymes.

Molecular Surface Properties—In cold-adapted enzymes, the accessible surface area is frequently characterized by a higher proportion of hydrophobic groups and an excess of negative charges. Although exposed hydrophobic groups are supposed to be entropically unfavorable, the excess of charge may improve interactions with the surrounding medium. However, there are few significant differences in the accessible surface properties of ColAP in terms of global hydrophobicity, polarity, or charge when compared with its mesophilic homologue (Table 3). Although theses surface properties display little correlation with those of other psychrophilic enzymes, it should be noticed that these results are in agreement with global trends

observed for proteins modeled from the genome of *C. psychrerythraea* (22). By contrast, the nature of the surface residues differs from those of the human enzyme, as ColAP exposes a higher proportion of aromatic residues to the solvent, as seen in several other cold-adapted proteins. Although it is generally accepted that a greater exposure of these groups results in entropic destabilization by weakening the hydrophobic effect, this may be also related to a lower entropic penalty cost at low temperatures. Indeed, at low temperatures, the cost of water structure ordering is reduced, which may favor the enhancement of aromatic and hydrophobic group exposure to the solvent (29).

Ion Pair Distribution and Complexity—Among the various molecular features suggested as determinants for protein thermal adaptation, electrostatic interaction optimization is considered a key mechanism. Several studies have shown that with increasing environmental temperature, ions pairs become more abundant in proteins and, in parallel, form networks of rising complexity (30–33). This aspect was investigated here by a survey of the electrostatic interactions in the psychrophilic ColAP and in the mesophilic LTH4A enzyme. Ions pairs were determined using three different criteria: (i) only Asp, Glu, Lys, and Arg side chains were considered; (ii) the maximal distance cutoff between charges was 4 Å; and (iii) adjacent residues in the primary structure were not retained if they formed a single ionic pair. Table 4 indicates that, as the number of ion pairs is similar in both enzymes, more difference can be seen in the nature of the residues implicated in these interactions. Although ions pairs are formed mainly by the interaction of Asp with Arg in ColAP, Asp tends to be replaced by Glu residues in the mesophilic enzyme. One should also note that for both enzymes, more than 60% of salt bridges include an Arg residue as the cation partner. Interestingly, the number

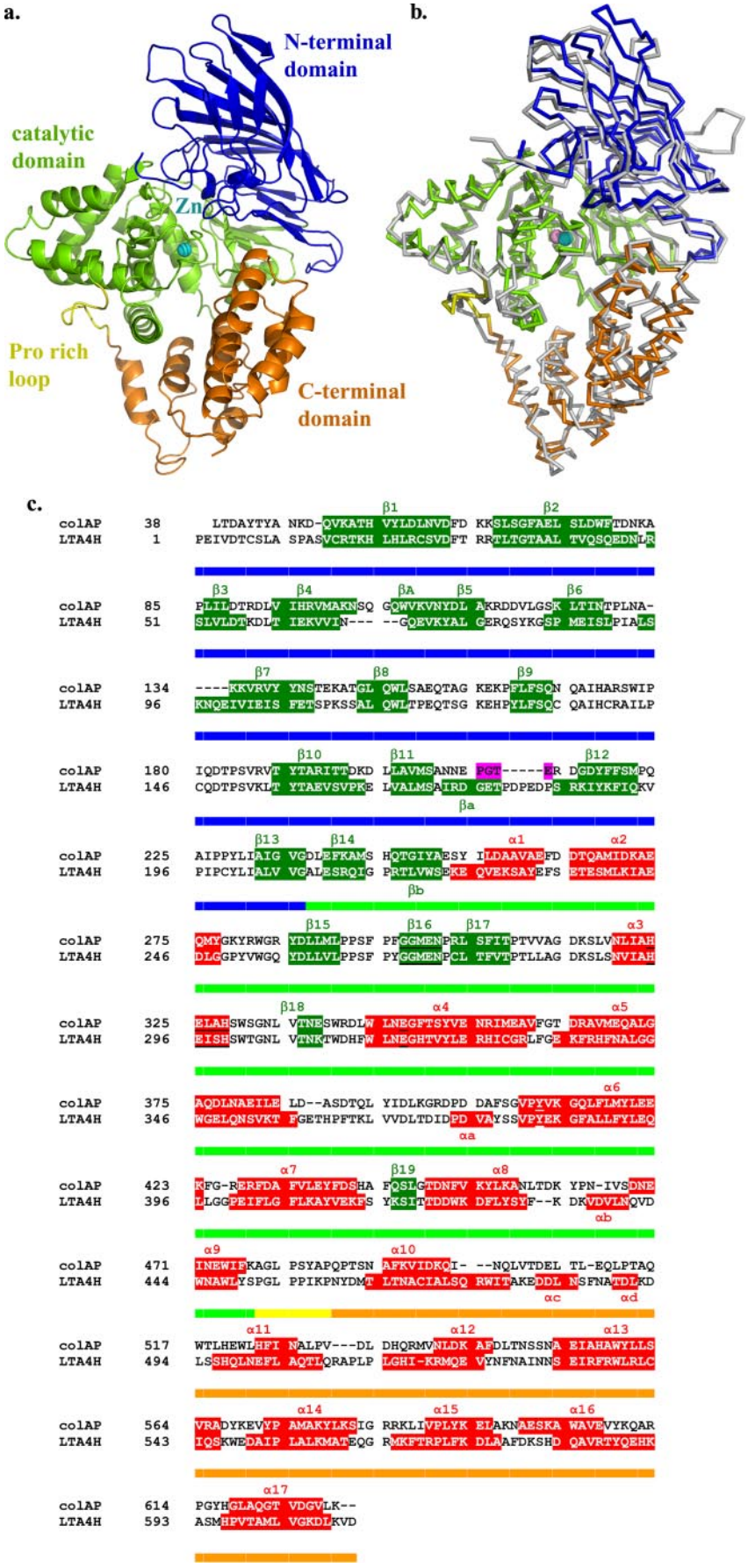

TABLE 2
Proportion of residues and computed chemical parameters in the psychrophilic ColAP and in human LTA4H

Amino acid composition	Amino acids	ColAP[a]		LTA4H		Frequency in Swiss-Prot[b]
		No.	Frequency	No.	Frequency	
			%		%	%
	Asp	46	7.6	34	5.6	5.3
	Glu	34	5.6	41	6.7	6.7
Negatively charged residues		*80*[c]	*13.2*	*75*	*12.3*	*12*
	Arg	22	3.6	23	3.8	5.4
	Lys	38	6.3	40	6.6	5.9
	His	15	2.5	16	2.6	2.3
Positively charged residues		*75*[c]	*12.4*	*79*	*13*	*13.6*
Total charged residues		*155*[c]	*25.6*	*154*	*25.3*	*25.6*
	Asn	32	5.3	21	3.4	4.1
	Gln	26	4.3	26	4.3	3.9
	Ser	34	5.6	45	7.4	6.8
	Thr	34	5.6	40	6.6	5.4
	Cys	0	0	11	1.8	1.5
	Tyr	30	5.0	22	3.6	3.0
Polar residues		*156*[c]	*25.8*	*165*	*27.0*	*24.7*
	Met	13	2.1	10	1.6	2.4
	Leu	63	10.4	69	11.3	9.6
	Ile	27	4.5	31	5.1	5.9
	Val	39	6.4	38	6.2	6.7
	Pro	25	4.1	35	5.7	4.8
	Ala	57	9.4	38	6.2	7.9
	Phe	26	4.3	27	4.4	3.9
	Trp	13	2.1	13	2.1	1.1
Nonpolar residues		*263*[c]	*43.5*	*261*	*42.8*	*42.3*
	Gly	31	5.1	30	4.9	7.0
Total number of residues		605		*610*		
Computed chemical parameters						
Molecular mass (Da)			68,593		69,154	
Theoretical pI			5.25		5.80	
Aliphatic index			86.2		88.2	
GRAVY index						
Total			−0.339		−0.259	
Strands			0.28		0.17	
Helices			−0.08		−0.21	
Loops			−0.75		−0.59	

[a] Peptide signal residues were omitted for calculation.
[b] See ExPASy Web site.
[c] Values in italic type correspond to the sum of amino acids gathered by type.

TABLE 3
Accessible surface area statistics

	Solvent-accessible surface area			
	ColAP		LTA4H	
	Å²	%	Å²	%
Primary structures				
Hydrophobic				
Ala, Ile, Phe, Leu, Met, Pro, Val	5,212	22.85	5,263	22.00
Polar				
Neutral polar				
Asn, Gln, Cys, Ser, Thr, Trp, Tyr	6,340	27.80	6,132	25.63
Basic residues				
Arg, Lys, His	5,546	24.32	6,117	25.57
Acidic residues				
Asp, Glu	5,137	22.52	5,877	24.56
Charged residues	10,683	46.84	11,994	50.13
Total	17,023	74.64	18,126	75.76
Glycine	572	2.51	537	2.24
Aromatic				
Phe, Trp, Tyr	1,891	8.29	1,359	5.68
Secondary structures				
α-Helices	6,445	28.26	7,812	32.65
β-Strands	3,647	15.99	4,965	20.75
Loops	12,715	55.75	11,149	46.60
Total accessible surface	22,807		23,926	

of complex ion pairs and of interdomain ion pairs is higher in the mesophilic LTH4A enzyme. No interdomain ion pair was found between the different ColAP domains, whereas five electrostatic interactions connect the N-terminal to the catalytic domains and the catalytic to the C-terminal domains of LTA4H. This indicates a higher level of interaction between domains in LTA4H than in ColAP. Finally, the ion pair repartition in the different domains differs in these two enzymes. In ColAP, 53% of the salt bridges are concentrated in the catalytic domain, whereas their repartition is homogenous all along the LTA4H domains. These results suggest that the localization and complexity of salt bridges are determining factors for ColAP thermal adaptation and that cohesion between the different domains is lower in the psychrophilic enzyme.

Hydrogen Bonding—Some psychrophilic enzymes are characterized by a decreased number of hydrogen bonds. Indeed, hydrogen bonds are a predominant factor for the folded state conformation (34), and consequently, a significant reduction in their number can contribute to a less stable structure. When

FIGURE 1. **Overall structure of ColAP.** The structural domains in ColAP are colored as follows: N-terminal domain in *blue* (residues 38–236), catalytic domain in *green* (residues 237–477), Pro-rich loops in *yellow* (residues 478–487), and C-terminal domain in *orange* (residues 488–629). *a*, backbone schematic diagram of the crystal structure of ColAP. *b*, superimposition of the Cα trace of ColAP and LTA4H (*gray*). *c*, structure-based sequence alignment performed with DEEPVIEW (18). β-Strands and α-helices are in *green* and *red*, respectively. Residues not seen in the structure are in *pink*. Conserved motif boxes are *underlined*. Conserved and nonconserved secondary structures are annotated using classical *Greek letters* (α and β for α-helices and β-strands, respectively) followed by a *number* or a *letter* if the structure is conserved or not, respectively.

TABLE 4

Composition, complexity, and localization of ion pairs in psychrophilic ColAP and in human LTA4H

Ion pairs	ColAP		LTA4H	
	No.	%	No.	%
Composition				
Asp-Arg	11	43	9	36
Glu-Arg	5	19	11	44
Glu-Lys	5	19	3	12
Asp-Lys	5	19	2	8
Total	26		25	
Complexity				
2 Residues	14		12	
3 Residues	6		3	
4 Residues	0		1	
5 Residues	0		1	
Localization				
N-terminal	8	31	6	24
Catalytic	13	50	8	32
C-terminal	5	19	6	24
Interdomain	0		5	20

TABLE 5

Hydrogen bonds in psychrophilic ColAP and in human LTA4H

Calculations were performed using HBPLUS.

	No. hydrogen bonds	No. hydrogen bonds/residues
ColAP (2.7 Å)[a]		0.86
Without water	502	
Water included (+306)	778	1.33
LTA4H (1.95 Å)[a]		1.01
Without water	618	
Water included (+551)	1345	2.20

[a] Resolution limits are shown in parentheses.

compared with LTA4H, ColAP is indeed characterized by a lower number of hydrogen bonds, whether or not water molecules are considered (Table 5). However, these variations may also arise from crystallographic artifacts such as differences in packing or in resolution limits. Actually, the number of hydrogen bonds is related to the protein fold but also depends on the solvation level, monomer arrangement in the crystal, and number of water molecules detected in the electronic density.

B-factors—The crystallographic temperature factor or "B-factor" measures the atomic agitation, which can be correlated to the uncertainty in atom position. Consequently, residues exhibiting more freedom are characterized by higher B-factor values. Hence, this experimental parameter gives an indication of the flexibility of the residues and regions of the protein structure. However, this parameter is affected by several crystallographic biases such as the refinement mode or molecular packing (30). To limit these artifacts and to compare different structures, it has been proposed that their relative B-factors rather than their absolutes values be compared (33, 35) after dividing the average temperature factors of the overall structure (32.2 and 29.2 $Å^2$ for ColAP and LTA4H, respectively). Fig. 2 displays the relative B-factor progress along the structure of both ColAP (*thick line*) and LTA4H (*thin line*) as well as the relative domain positions. In these enzymes, no clear divergence was seen between the catalytic domain relative B-factors except for some minor differences (Table 6). Surprisingly, the ColAP N-terminal domain presents a global lower relative B-factor than the equivalent domain in LTA4H, with average relative B-factors of about 0.75 and 1.37 $Å^2$ for ColAP

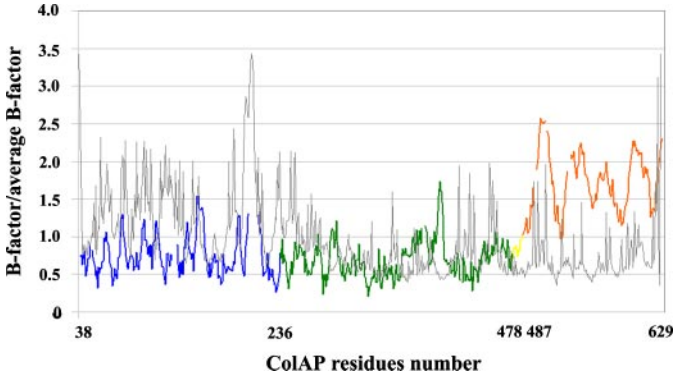

FIGURE 2. **Relative B-factors for ColAP (*thick line*) and LTA4H (*thin gray line*).** The different ColAP domains are represented in *blue* (N-terminal), *green* (catalytic), and *orange* (C-terminal). The Pro-rich loop position is in *yellow*.

TABLE 6

Relative B-factor for the structural domains in the psychrophilic ColAP and in human LTA4H

The number of atoms in the domains is given in parentheses.

Domain	Relative B-factor	
	ColAP	LTA4H
N-Terminal	0.75 (1552)	1.37 (1604)
Catalytic	0.69 (1948)	0.82 (1980)
Pro-rich loop	0.84 (70)	0.59 (77)
C-Terminal	1.73 (1138)	0.72 (1215)

and LTA4H N-terminal domains, respectively. This lower flexibility in ColAP originates from segments homogeneously distributed along the N-terminal domain and is characterized by a low relative B-factor. By contrast, the ColAP C-terminal domain is more flexible, with relative B-factors of 1.73 and 0.72 $Å^2$ for ColAP and LTA4H C-terminal domains, respectively. These high relative B-factor values arise from all C-terminal domain residues in ColAP and begin in the Pro-rich loop equivalent (Fig. 2). This indicates that the whole C-terminal domain presents a high plasticity, which may be tentatively related to the lack of interdomain ion pairs, to the low number of intradomain salt bridges, and to a less constrained Pro-rich loop equivalent. It is worth mentioning that such differential distribution of B-factors between domains has been reported for a psychrophilic citrate synthase (36) and that distinct domain stabilities have been demonstrated by microcalorimetric studies of some cold-adapted enzymes (37, 38).

It seems, therefore, that differential domain flexibilities could be involved in the temperature adaptation of ColAP. It has been hypothesized that, in multidomain psychrophilic enzymes, a flexible domain may contribute to an improved activity at low temperatures, whereas maintenance of a compact and stable domain could provide tight substrate binding. Interestingly, ColAP displays both high activity and substrate affinity at low temperature in comparison with LTA4H (ColAP k_{cat} = 15.8 s^{-1}, K_m = 2.3 mM; LTH4A k_{cat} = 1.9 s^{-1}, K_m = 10.8 mM at 10 °C, with L-alanine-4-nitroanilide as substrate (4)), which can be related tentatively to its distinct B-factors by domain. In this context, it should be noted that both the N- and C-terminal domains bear residues forming the catalytic cavity. From a thermodynamic point of view, it has also been argued that a compact domain could balance the rise in conformational entropy of the flexible domain (39).

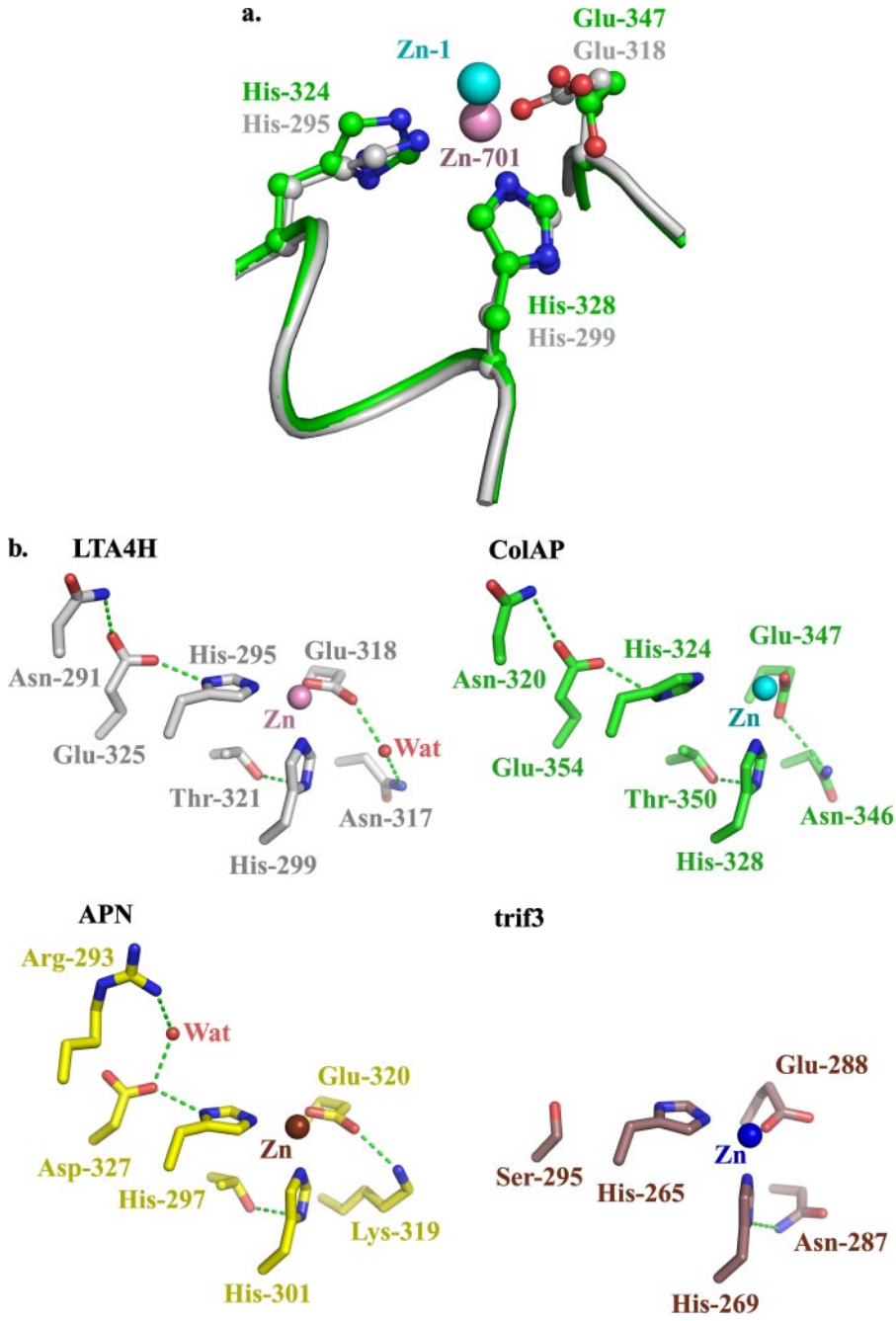

FIGURE 3. **Metal coordination comparison between ColAP and other M1 family members.** *a*, superimposition of zinc ligand binding residues of both ColAP (*green*) and LTA4H (*gray*). Ligand residues are shown in a *ball-and-stick* representation and zinc cations as a *cyan* and a *blue sphere* for ColAP and LTA4H, respectively. *b*, comparison of metallic second coordination sphere for different M1 family members: LTA4H (*gray*), ColAP (*green*), APN (*yellow*), trif3 (*brown*). H-bonds are represented by *green dashed lines*. The catalytic zinc ions are shown as *pink*, *cyan*, *brown*, and *blue spheres* for LTA4H, ColAP, APN, and trif3, respectively. A water molecule (*Wat*) is represented as a *red sphere*.

Metal Binding Site—As the others members of M1 metallopeptidase family (MEROPS peptide data base, (40)), the amino acid sequence ColAP is characterized by the conserved motif ^{324}HE*XX*H^{328} in which the histidine residues are the first two ligands of the metallic atom. The third ligand corresponds to a glutamate residue (Glu-347) and is found toward the C terminus. Superimposition of both the LTA4H and ColAP metal binding motifs clearly indicates that the three ligand residues are located at equivalent positions and that secondary structure, including those residues, fits very well for the most part (Fig. 3*a*).

It has been proposed that in enzymes sharing this zinc binding motif, the second coordination sphere of zinc is less well conserved (41). This was corroborated by observations made on crystal structures of enzymes belonging to the M1 family such as APN (21), Tricorn protease-interacting factor f3 (trif3) (20), and LTA4H (2) enzymes (Fig. 3*b*). Indeed, although in LTA4H the first ligand (His-295) is stabilized by a glutamate (Glu-325), which further interacts with an asparagine (Asn-291), in APN similar interactions occurred among His-297, Asp-327, and Arg-293, with these two last residues interacting via a water molecule. In the trif3 enzyme, the residue corresponding to Glu-325 in LTA4H is a serine (Ser-295) in which the side chain is too short to interact with the first ligand residue (His-265). The second ligand, the histidine (His-299, His-269, and His-301 for LTA4H, trif3, and APN, respectively), may be stabilized either by a threonine as observed in LTA4H (Thr-321) and APN (Thr-323) enzymes or by an asparagine (Asn-287) as observed for trif3. Regarding the third ligand, the glutamate bounded to the zinc further interacts directly with a lysine (Lys-319) in APN or, as for LTA4H, via a water molecule to an asparagine (Asn-317). In trif3, there is no water molecule preventing Glu-288 from connecting to Asn-287. The second coordination sphere of zinc may consequently be informative of how two gluzincin enzymes (metalloproteases defined by the HE*XX*H motif and having a glutamic acid as the third zinc ligand (42)) are structurally close. In ColAP and LTA4H, the environments of canonical zinc binding residues are nearly identical. All of the implicated residues are conserved in their natures and positions in both enzymes, and the only difference corresponds to the absence in ColAP of a water molecule between Glu-347 and its neighbor residue, Asn-346. This part of the active site is thus particularly well conserved in these two enzymes.

In ColAP, a high electronic density is located near the three ligand residues, which cannot be explained by the presence of a

water molecule or by any component of crystallization solution. Additionally, the x-ray fluorescence spectrum confirmed the presence of a zinc ion in the crystallographic sample (data not shown). These results suggest that the high density found in ColAP could correspond to a zinc cation located in the metal binding site. However, significant differences are observed between ColAP and LTA4H metal coordination geometry. Although in the human enzyme, the zinc cation is located at 1.96, 2.05, and 1.93 Å from His-295, His-299, and Glu-318, respectively, the metallic atom in ColAP is more distant at 2.99, 2.65, and 2.8 Å from the corresponding residues (His-324, His-328, and Glu-347, respectively). These distances are similar in LTA4H in the presence and in absence of inhibitor. Consequently, the differences between these two enzymes cannot be related to ligand binding. One also notes the absence of the fourth ligand, resulting in unusual coordination geometry for such metallic cofactor. Furthermore, the differences are also noticeable regarding the side chains of the zinc ligands. In the two enzymes, ligand side chains are directed toward the metallic ion. However, as the metallic atoms are not found at equivalent locations, the ligand side chains present slight differences in their conformations. Hence, the carboxylate and imidazole groups of Glu-347 and His-324 of ColAP form an angle around 90 and 30° relative to their equivalents in human enzyme (Fig. 3*a*). Finally, in contrast to observations made on different LTA4H structures, zinc cation occupancies are partial, between 30 and 40% depending on the ColAP monomer considered. The atypical geometry of the metallic center observed in ColAP could be correlated to this poor site occupancy, giving an altered average image rising from crystallographic juxtaposition of active sites in diverse situations, for example active sites in both the presence or absence of zinc cation. Furthermore, the 2.7 Å resolution of the ColAP structure does not allow a precise determination of the amino acid-zinc cation distances. Nevertheless, although the sources of such binding site configurations presently remain unexplained and require further investigation, these data suggest that zinc affinity is probably weaker in ColAP than in its mesophilic counterpart. It should be noted that all psychrophilic proteins investigated thus far display low binding affinities for metal ions (43, 44).

Aminopeptidase Active Site—On the basis of studies made on LTA4H and related monozinc aminopeptidase, several residues have been shown to be implicated into the catalytic mechanism. Among those residues, some are required for the scissile bond rupture, such as a glutamate (Glu-296 in LTA4H) and a tyrosine (Tyr-383 in LTA4H) presumably as general base and proton donor, respectively (41, 45). Others residues confer to those enzymes their exopeptidase specificity as a glutamate included in the G*X*MEN conserved motif (Glu-271 in LTA4H) probably assisted by a glutamine residue in LTA4H (Gln-136) (41, 45–47). Positively charged residues were also found to stabilize the substrate in the active site by interacting with its C-terminal carboxylate. In LTA4H, this function is exerted by a couple of residues, Arg-563 and Lys-565 (46). Finally, some residues forming a hydrophilic cluster inside the LTA4H active site (namely Gln-134, Asp-375, and Tyr-267) are involved in the substrate specificity. They provide a negative charge to the N-terminal side chain residue of the substrate and confer to the enzyme its preference for a peptidic substrate starting with an arginine (2).

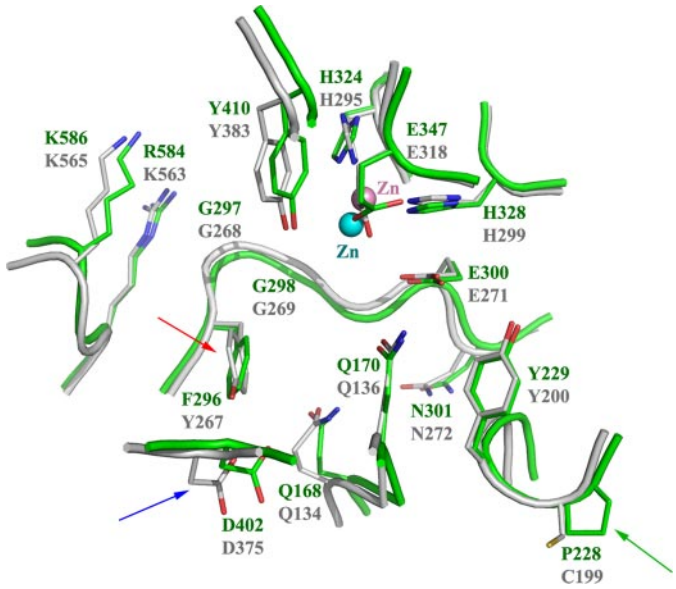

FIGURE 4. **ColAP and LTA4H aminopeptidase active sites.** The superimposition of ColAP (*green*) and LTA4H (*gray*) aminopeptidase active sites is shown. The Cα trace and catalytic residue side chain are shown as a *smooth ribbon* and a *stick*, respectively. The metallic cations are represented by a *pink* and a *cyan sphere* for ColAP and LTA4H, respectively. Differences are indicated by *arrows*.

Interestingly, in ColAP, both the nature and position of all of those catalytic residues were found to be conserved in the structure. The conservation of functional groups found in a similar arrangement suggests that corresponding residues have similar functions in both human and psychrophilic enzymes. Consequently, by analogy with LTA4H and related aminopeptidases, we suggest that ColAP aminopeptidase activity also follows a zinc-assisted general base mechanism. Several residues included in the ^{297}GGMEN ColAP motif would be implicated in both binding and alignment of substrate. As proposed previously for the corresponding Glu-271 in LTA4H, Glu-350 in APN, and Glu-352 for aminopeptidase A, Glu-300, probably assisted by Asn-301/Gln-170, would interact with the free N-terminal substrate conferring its exopeptidase specificity to ColAP. Further interactions could be made between the substrate and main chain atoms of Gly-297 and Gly-298. Arg-584 and Lys-586, corresponding to Arg-563 and Lys-565 in LTA4H, respectively, would be involved in recognizing the C terminus of substrate and could limit the substrate length. It should be noticed that the distances between Glu-300 and both Arg-563 and Lys-565 are nearly identical when compared with the equivalents in LTA4H. As these distances were suggested previously as an important determinant for the tripeptide specificity of LTA4H (46), we suggest that ColAP has the same preference for tripeptide substrates. More significant differences can be observed for the hydrophilic cluster. A phenylalanine was found in ColAP in position 296 instead of a tyrosine in LTA4H (Tyr-267) (Fig. 4, *red arrow*). Furthermore, Asp-402, corresponding to Asp-375 of LTA4H, has moved into the active site by ~1 Å about one angstrom (Fig. 4, *blue arrow*). However, the net charge supposed to interact with the guanidinium head

group of arginine substrates as well as the corresponding glutamine residues of the hydrophilic cluster, Gln-134 in LTA4H and Gln-168 in ColAP, respectively, is conserved in both the psychrophilic and mesophilic enzymes. This may be correlated to the fact that the two enzymes show the same preference for arginine substrates (1). Indeed, this suggests that these differences have very little influence on the peptide specificity of these enzymes and confirms that the presence of a negative charge in this active side pocket is a determinant for this enzyme specificity.

In such a binding mode, the oxygen carbonyl of the scissile bond would be located near the zinc cation, and a water molecule polarized by the metallic cofactor and Glu-300 would be able to make a nucleophilic attack on the carbonyl. A carbocation would thus be generated in which the charge would be stabilized by interactions with the zinc cation, Glu-300, Glu-347, and maybe Tyr-229. Indeed, Thompson *et al.* (48) have recently shown that mutation in phenylalanine of the corresponding Tyr-244 of yeast LTA4H drastically reduces the catalytic activity. They also established the key function of this residue in transition state stabilization (48). Because this residue is too far away to interact directly with any substrate, the same authors suggested that there is a displacement of the loop harboring the tyrosine that leads it in position to interact with the transition state (48). It should be noted that the corresponding loops in human LTA4H and ColAP, residues 198–202 and 227–231, respectively, are well conserved except for the supplementary proline in psychrophilic enzyme (Cys-119 replaced by Pro-228; *green arrow* in Fig. 4). Finally, in the last step of the mechanism, Tyr-410 could act as a proton donor, and the products would then be released.

Epoxide Hydrolase Active Site—In addition to its aminopeptidase activity, human LTA4H retains the particularity of being an epoxide hydrolase with the ability to convert LTA4 into LTB4, a lipidic chemoattractant involved in inflammation (Fig. 5). This second highly specific reaction also requires the zinc cation and occurs in an overlapping active site (49). As a result of hydrolysis, the epoxide moiety is broken and a hydroxyl group is stereospecifically introduced at C-12 of the substrate (Fig. 5). This is made possible only via a precise positioning of LTA4 in the active site, as a very accurate geometry and distribution of polar and hydrophobic groups inside this active site (3, 47). According to the generally accepted model, the fatty acid substrate LTA4 adopts a curved general conformation with its carboxylate group interacting with Arg-563. This interaction would place the oxirane ring near the zinc ion and the C-12 in the proximity of a water molecule bound to Asp-375, which is supposed to be responsible for the stereoselective insertion of the 12*R*-hydroxyl group in LTB4. Finally, the C-7—C-20 olefinic tail would be enclosed more deeply in a narrow pocket formed principally by two protein segments (residues 360–379 and 308–320). In agreement with this model, Haeggstrom *et al.* (45, 49) have suggested that in the human LTA4H, some residues, such as Glu-296 and Tyr-383, are needed specifically for aminopeptidase activity and other residues, such as Glu-271 and Arg-563, are implicated in the two reactions. In addition, a single residue, Asp-375, has been demonstrated to be specific for epoxide reaction (2).

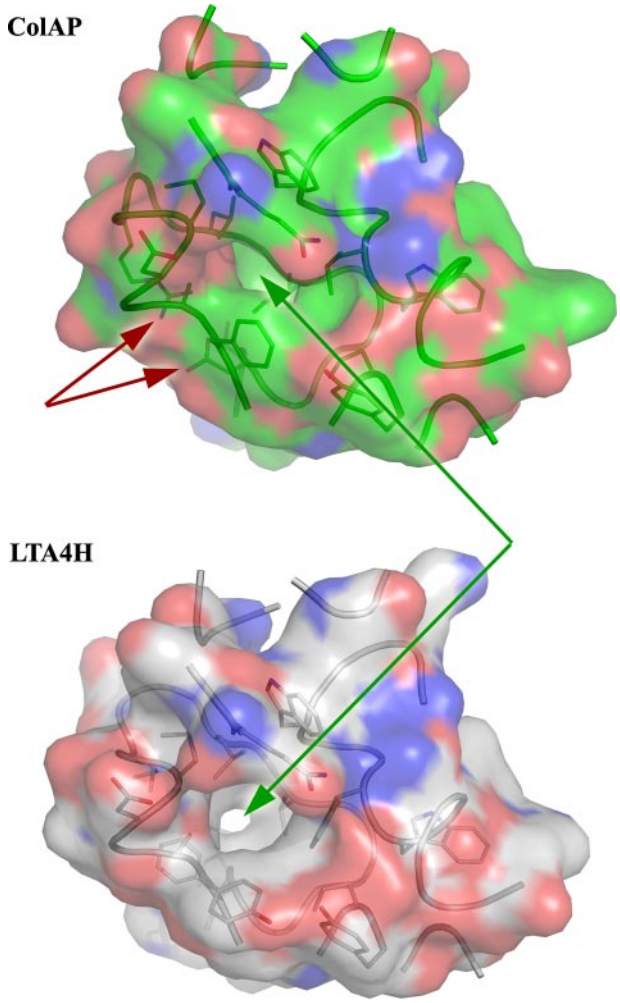

FIGURE 5. **Accessibility comparison of olefinic substrate binding region.** The semitransparent molecular surface of LTA4H (*gray*) allows one to see the backbone (*smooth* schematic) and the side chains (*sticks*) of residues surrounding the suggested olefinic binding pocket. The corresponding pocket in ColAP is displayed in *green*. Major differences are indicated by *arrows*.

As shown previously, the aminopeptidase active sites of ColAP and LTA4H enzymes are very similar. This is not the case for the part of the active site supposed to be more specific for the LTA4 hydrolyzes. As already seen, Asp-402, corresponding to the essential Asp-375 in LTA4H, is displaced from ~1 Å (Fig. 4, *blue arrow*). Furthermore, its hydrophilic environment is only partially conserved. As shown in Fig. 6, further differences are observed between the hypothetical olefinic tail binding pockets. The main chain of residues 394–399, corresponding to residues 367–372 in LTA4H, adopts a different conformation and occludes the pocket (opened to solvent in the human enzyme). This is probably due to the presence of an additional salt bridge formed between Arg-399 (Ile-372 in LTA4H) and Asp-389 (Phe-362 in LTA4H) (Fig. 6, *red arrows*) and of a glycine in position 398 (Asp-371 in LTA4H). Also, in ColAP, the Ile-394 side chain (Val-367 in LTA4H) points directly inside the pocket (Fig. 6, *green arrows*). These differences suggest that ColAP is probably unable to bind and perhaps hydrolyze LTA4.

Concluding Remarks—In this article we have reported the first cold-adapted structure of a member of the M1 metallopep-

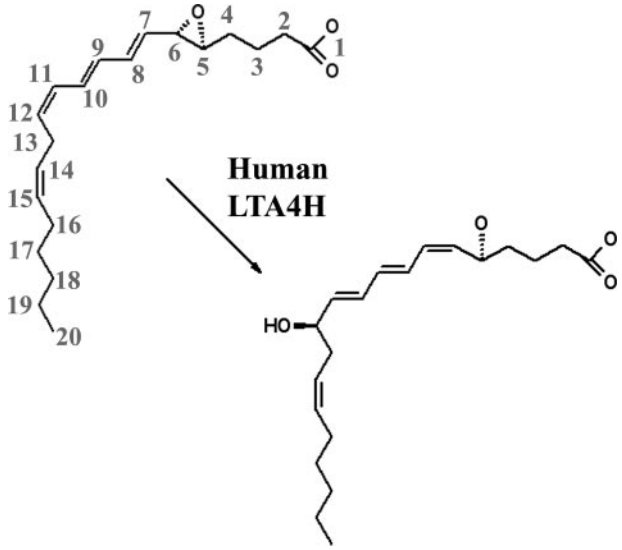

FIGURE 6. **Epoxide hydrolysis reaction catalyzed by human LTA4H.**

tidase family, ColAP. Its nearest structural homologue is the human LTA4H, a bifunctional enzyme, which, in addition to being an aminopeptidase, is able to hydrolyze the epoxide moiety of LTA4 and convert it into LTB4. The extensive structural analysis made on these two enzymes has highlighted several determining factors implicated in the adaptation to a cold environment. The Ala content is higher in ColAP and seems to be correlated to a reduction of more aliphatic residues, suggesting a global decrease in packing. Additionally, we observed an increase in loop lengths associated with a reduction of regular secondary structure, suggesting an increase in the resilience of the molecular surface of ColAP. Finally, a decreased interdomain cohesion (principally observed for C-terminal domain) was observed, which may be correlated in part to a weakening of the electrostatic interactions. Although all of the reported parameters are expected to be structural determinants of enzyme temperature adaptation, one cannot rule out the possibility that some of them also may be related to the ecological and physiological differences between both source organisms.

In agreement with their similar catalytic specificities, a comparison of the aminopeptidase active sites revealed that they are nearly identical. This strongly suggests that the catalytic mechanism is conserved in these two homologues. This is not the case for the olefinic LTA4 binding region, which differs significantly in both enzymes, suggesting that the aminopeptidase active site has evolved from a common ancestor and that the second activity of LTA4H appeared later by the reshaping of the lipidic binding region.

Acknowledgments—We thank C. Legrain, E. Jacobs, A. Royant, and P. Carpentier for very useful discussion.

REFERENCES

1. Huston, A. L., Methe, B., and Deming, J. W. (2004) *Appl. Environ. Microbiol.* **70,** 3321–3328
2. Rudberg, P. C., Tholander, F., Thunnissen, M. M., and Haeggstrom, J. Z. (2002) *J. Biol. Chem.* **277,** 1398–1404
3. Thunnissen, M. M., Nordlund, P., and Haeggstrom, J. Z. (2001) *Nat. Struct. Biol.* **8,** 131–135
4. Huston, A. L., Haeggstrom, J. Z., and Feller, G. (2008) *Biochim. Biophys. Acta*, in press
5. Roth, M., Carpentier, P., Kaikati, O., Joly, J., Charrault, P., Pirocchi, M., Kahn, R., Fanchon, E., Jacquamet, L., Borel, F., Bertoni, A., Israel-Gouy, P., and Ferrer, J. L. (2002) *Acta Crystallogr. Sect. D Biol. Crystallogr.* **58,** 805–814
6. Kabsch, W. (1993) *J. Appl. Crystallogr.* **26,** 795–800
7. Weiss, M. (2001) *J. Appl. Crystallogr.* **34,** 130–135
8. Evans, P. (2006) *Acta Crystallogr. Sect. D Biol. Crystallogr.* **62,** 72–82
9. Jones, T. A., Zou, J. Y., Cowan, S. W., and Kjeldgaard, M. (1991) *Acta Crystallogr. Sect. A* **47,** 110–119
10. Emsley, P., and Cowtan, K. (2004) *Acta Crystallogr. Sect. D Biol. Crystallogr.* **60,** 2126–2132
11. Brunger, A. T., Adams, P. D., Clore, G. M., DeLano, W. L., Gros, P., Grosse-Kunstleve, R. W., Jiang, J. S., Kuszewski, J., Nilges, M., Pannu, N. S., Read, R. J., Rice, L. M., Simonson, T., and Warren, G. L. (1998) *Acta Crystallogr. Sect. D Biol. Crystallogr.* **54,** 905–921
12. Murshudov, G. N., Vagin, A. A., and Dodson, E. J. (1997) *Acta Crystallogr. Sect. D Biol. Crystallogr.* **53,** 240–255
13. Gasteiger, E., Gattiker, A., Hoogland, C., Ivanyi, I., Appel, R. D., and Bairoch, A. (2003) *Nucleic Acids Res.* **31,** 3784–3788
14. Lovell, S. C., Davis, I. W., Arendall, W. B., 3rd, de Bakker, P. I., Word, J. M., Prisant, M. G., Richardson, J. S., and Richardson, D. C. (2003) *Proteins* **50,** 437–450
15. Hooft, R. W., Vriend, G., Sander, C., and Abola, E. E. (1996) *Nature* **381,** 272
16. Kabsch, W., and Sander, C. (1983) *Biopolymers* **22,** 2577–2637
17. McDonald, I. K., and Thornton, J. M. (1994) *J. Mol. Biol.* **238,** 777–793
18. Guex, N., and Peitsch, M. C. (1997) *Electrophoresis* **18,** 2714–2723
19. Weng, Z., Rickles, R. J., Feng, S., Richard, S., Shaw, A. S., Schreiber, S. L., and Brugge, J. S. (1995) *Mol. Cell. Biol.* **15,** 5627–5634
20. Kyrieleis, O. J., Goettig, P., Kiefersauer, R., Huber, R., and Brandstetter, H. (2005) *J. Mol. Biol.* **349,** 787–800
21. Ito, K., Nakajima, Y., Onohara, Y., Takeo, M., Nakashima, K., Matsubara, F., Ito, T., and Yoshimoto, T. (2006) *J. Biol. Chem.* **281,** 33664–33676
22. Methe, B. A., Nelson, K. E., Deming, J. W., Momen, B., Melamud, E., Zhang, X., Moult, J., Madupu, R., Nelson, W. C., Dodson, R. J., Brinkac, L. M., Daugherty, S. C., Durkin, A. S., DeBoy, R. T., Kolonay, J. F., Sullivan, S. A., Zhou, L., Davidsen, T. M., Wu, M., Huston, A. L., Lewis, M., Weaver, B., Weidman, J. F., Khouri, H., Utterback, T. R., Feldblyum, T. V., and Fraser, C. M. (2005) *Proc. Natl. Acad. Sci. U. S. A.* **102,** 10913–10918
23. Lee, D. Y., Kim, K. A., Yu, Y. G., and Kim, K. S. (2004) *Biochem. Biophys. Res. Commun.* **320,** 900–906
24. Medigue, C., Krin, E., Pascal, G., Barbe, V., Bernsel, A., Bertin, P. N., Cheung, F., Cruveiller, S., D'Amico, S., Duilio, A., Fang, G., Feller, G., Ho, C., Mangenot, S., Marino, G., Nilsson, J., Parrilli, E., Rocha, E. P., Rouy, Z., Sekowska, A., Tutino, M. L., Vallenet, D., von Heijne, G., and Danchin, A. (2005) *Genome Res.* **15,** 1325–1335
25. Schiffer, C. A., and Dotsch, V. (1996) *Curr. Opin. Biotechnol.* **7,** 428–432
26. Siddiqui, K. S., and Cavicchioli, R. (2006) *Annu. Rev. Biochem.* **75,** 403–433
27. Chakravarty, S., and Varadarajan, R. (2002) *Biochemistry* **41,** 8152–8161
28. Riise, E. K., Lorentzen, M. S., Helland, R., Smalas, A. O., Leiros, H. K., and Willassen, N. P. (2007) *Acta Crystallogr. Sect. D Biol. Crystallogr.* **63,** 135–148
29. Arnorsdottir, J., Kristjansson, M. M., and Ficner, R. (2005) *FEBS J.* **272,** 832–845
30. Aghajari, N., Feller, G., Gerday, C., and Haser, R. (1998) *Structure* (*Lond.*) **6,** 1503–1516
31. Bell, G. S., Russell, R. J., Connaris, H., Hough, D. W., Danson, M. J., and Taylor, G. L. (2002) *Eur. J. Biochem.* **269,** 6250–6260
32. Karshikoff, A., and Ladenstein, R. (2001) *Trends Biochem. Sci.* **26,** 550–556
33. Violot, S., Aghajari, N., Czjzek, M., Feller, G., Sonan, G. K., Gouet, P., Gerday, C., Haser, R., and Receveur-Brechot, V. (2005) *J. Mol. Biol.* **348,** 1211–1224
34. Creighton, T. E. (1991) *Curr. Biol.* **1,** 8–10

35. Van Petegem, F., Collins, T., Meuwis, M. A., Gerday, C., Feller, G., and Van Beeumen, J. (2003) *J. Biol. Chem.* **278,** 7531–7539
36. Russell, R. J., Gerike, U., Danson, M. J., Hough, D. W., and Taylor, G. L. (1998) *Structure* (*Lond.*) **6,** 351–361
37. Zecchinon, L., Oriol, A., Netzel, U., Svennberg, J., Gerardin-Otthiers, N., and Feller, G. (2005) *J. Biol. Chem.* **280,** 41307–41314
38. Suzuki, Y., Takano, K., and Kanaya, S. (2005) *FEBS J.* **272,** 632–642
39. Lonhienne, T., Gerday, C., and Feller, G. (2000) *Biochim. Biophys. Acta* **1543,** 1–10
40. Rawlings, N. D., Morton, F. R., and Barrett, A. J. (2006) *Nucleic Acids Res.* **34,** D270–272
41. Thunnissen, M. M., Andersson, B., Samuelsson, B., Wong, C. H., and Haeggstrom, J. Z. (2002) *FASEB J.* **16,** 1648–1650
42. Hooper, N. M. (1994) *FEBS Lett.* **354,** 1–6
43. Feller, G., Payan, F., Theys, F., Qian, M., Haser, R., and Gerday, C. (1994) *Eur. J. Biochem.* **222,** 441–447
44. Feller, G., d'Amico, D., and Gerday, C. (1999) *Biochemistry* **38,** 4613–4619
45. Haeggstrom, J. Z., Tholander, F., and Wetterholm, A. (2007) *Prostaglandins Other Lipid Mediat.* **83,** 198–202
46. Rudberg, P. C., Tholander, F., Andberg, M., Thunnissen, M. M., and Haeggstrom, J. Z. (2004) *J. Biol. Chem.* **279,** 27376–27382
47. Tholander, F., Kull, F., Ohlson, E., Shafqat, J., Thunnissen, M. M., and Haeggstrom, J. Z. (2005) *J. Biol. Chem.* **280,** 33477–33486
48. Thompson, M. W., Archer, E. D., Romer, C. E., and Seipelt, R. L. (2006) *Peptides* (*Elmsford*) **27,** 1701–1709
49. Haeggstrom, J. Z. (2004) *J. Biol. Chem.* **279,** 50639–50642